Theoretical Investigations of (Oxidative) Dehydrogenation of Propane to Propylene over Palladium Surfaces

Eduard Araujo-Lopez, Lennart Joos, Bart D. Vandegehuchte, Dmitry I. Sharapa, and Felix Studt*

ABSTRACT: Herein, we present density functional theory calculations of the (oxidative) dehydrogenation of propane on Pd(111) and Pd(211) surfaces. We find that, independently of the surfaces and the intermediate product (1 propyl or 2 propyl), O assisted dehydrogenation of propane is always less favorable than the direct or OH assisted hydrogen abstraction. Additionally, we show that the transition state energies of the (oxidative) dehydrogenation of propane on Pd surfaces scale with the final state energies and are similar to trends observed for methane activation. This work is a first and essential step to understand the role of surface oxygen species and the mechanism of (O)DHP on Pd based catalysts.

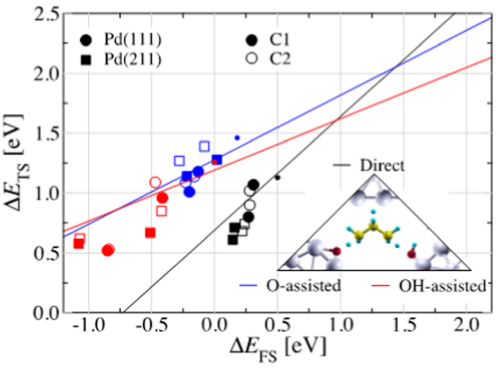

■ INTRODUCTION

The markets for propylene derivatives have grown rapidly over the last few years and are likely to continue doing so.[1,2] This demand is thought to be met by dehydrogenation of propane (DHP), with variants thereof being oxidative dehydrogenation using O_2 (ODHP)[3,4] or CO_2 (CO_2 ODHP).[5−7] Although the ODHP in the presence of molecular O_2, as an oxidizing agent, favors low temperature reactions and is exothermic, deep oxidation to CO_x is a major drawback, which often results in loss of propylene selectivity and yield. To circumvent these issues, milder oxidants such as CO_2 are also explored.[8]

Among the many catalysts tested for the DHP are supported metal particles such as platinum,[9,10] nickel,[11,12] and palladium,[13,14] whereas metal oxides, such as chromium oxide,[15] vanadium oxide,[16,17] and gallium oxide,[18] but also carbon based materials[3] and zeolites[19] have been proposed for ODHP. Among metal based catalysts, only platinum has advanced to commercial applications of the DHP thanks to its superior activation of paraffinic C−H bonds and low activity toward undesired C−C cleavage.[7] The high cost of Pt as well as poisoning of the active sites by coke at high temperatures (showing poor propylene selectivity and fast deactivation) are the main limitations of the Pt based catalysts.[20]

Studies on palladium based catalysts, on the other hand, have been scarce, although interest in these catalysts has increased in recent years.[13,14,21−23] Recently, Nowicka et al.[13] synthesized a Pd/$CeZrAlO_x$ material for CO_2−ODHP with long term stability and, high activity and selectivity. Additionally, selective DHP catalysts of PdM (M = Zn, In, Fe) alloys for olefin production showing improved stability compared to bare Pd nanoparticles have been reported.[14,22−24] These studies suggest that the isolation of active metal sites by inactive atoms is responsible for high olefin selectivity, as it has been reported before for PtSn alloys.[25]

While the reaction mechanism of DHP on Pt based catalysts has been the subject of many computational studies,[20,26−28] theoretical investigations targeting Pd based catalysts have not been reported to date. Herein, we report a mechanistic study of DHP and ODHP over palladium (111) and (211) surfaces using density functional theory (DFT) calculations. We show the mechanism by which propane is converted into propylene, how the structure of the metal surface is influencing activity, and we explore the role of surface oxygen that would be present in ODPH.

■ COMPUTATIONAL METHODS

DFT calculations were carried out using the Vienna Ab Initio Simulation Package (VASP)[29,30] and the Atomic Simulation Environment (ASE)[31] employing the generalized gradient approximation (GGA) using the Bayesian error estimation functional with van der Waals corrections (BEEF−vdW)[32,33] and the projector augmented wave (PAW) potentials.[34,35] The choice of the BEEF−vdW functional is motivated by its performance with respect to adsorption energies[36] and transition states[37] on transition metal surfaces. The kinetic energy cutoff and the k point mesh were 450 eV and 4 × 4 × 1,

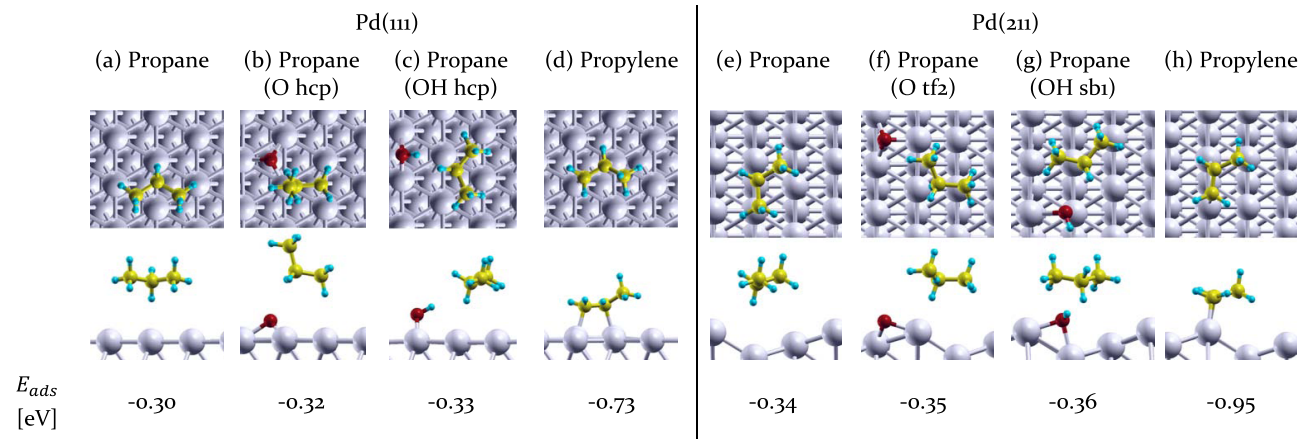

Figure 1. Top and side views of the most stable configurations of propane (a, e) on clean, (b, f) oxygen preadsorbed, (c, g) hydroxyl preadsorbed; and (d, h) propylene over Pd(111)/Pd(211) surfaces.

Scheme 1. Reaction Mechanism of DHP (Black) and Oxygen Assisted DHP (ODHP, Blue/Red)[a]

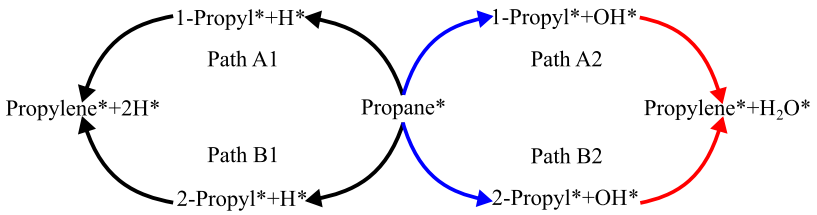

[a]The color code used in this scheme (black, blue, and red lines/markers represent the direct, O , or OH assisted dehydrogenation of C_xH_y species) is the same as in all of the other figures.

respectively. When specified, single point calculations were performed using the PBE functional including Grimme's dispersion corrections (PBE + D3) using the same parameters.[38,39]

Four layer slabs with $p(3 \times 3)$ and $p(1 \times 3)$ supercells are used to represent the palladium (111) and (211) surfaces, with dimensions of 8.44 × 8.44 and 6.89 × 8.44 Å, respectively (see Figure S1). The two bottom layers of the slabs were fixed during the relaxations. To avoid interaction between periodic images, the Pd slabs are separated by ∼15 Å of vacuum along the z direction. To investigate possible interactions between periodic images, we used bigger supercells with four layer slabs, and sizes of (4 × 4) and (6 × 6) for the Pd(111) and Pd(211) surfaces (the k points meshed were 3 × 3 × 1 and 2 × 2 × 1), respectively.

The adsorption energy is defined as follows:

$$E_{ads} = E_{X+surf} - E_X - E_{surf} \quad (1)$$

In eq 1, all energies refer to systems with optimized structures; E_{X+surf} stands for the total energy of the molecule/species adsorbed, E_X is the energy of the adsorbate calculated in the gas phase, and E_{surf} is the energy of the slab. By this definition, a negative value corresponds to an exothermic process. The isolated molecules involved in the propane (oxidative) dehydrogenation process (propane, hydrogen, propylene, water, and CO_2) were structurally relaxed inside a large simulation box of 15 × 15 × 15 Å^3.

The transition state (TS) searches along the reaction path were systematically performed using the nudge elastic band (NEB)[40] and DIMER[41] methods at the same theoretical level as those for the reactants and products. The structures used to search the TS in each dehydrogenation step were chosen based on the most stable adsorptions of C_3 compounds over the preadsorbed oxygen species. The final TS structures were confirmed by a single imaginary frequency along the reaction coordinate calculated with a normal mode analysis by using a finite difference approximation of the Hessian matrix.

The thermochemistry module from ASE was used to obtain zero point energy (ZPE) and entropy (S) contributions, and temperature variations using C_P for the Gibbs free energy. The gas phase molecules and the palladium surfaces (with or without preadsorbed oxygen species) were taken as reference values, as illustrated in Figure S2. For all adsorbates and TS, the calculations were done under the harmonic limit and the values for the gas phase molecules were taken from experimental data or the NIST database.[42−44]

RESULTS AND DISCUSSION

The calculated propane adsorption energies on Pd(111) and Pd(211) were −0.30 and −0.34 eV, respectively. This compares to the experimentally measured value of −0.46 eV for the Pd(111) surface[45] and presents an error of the same order of magnitude as that obtained for propane adsorption on other surfaces such as Pt.[25,46] The differences in energy (for the adsorptions and transition states of C_3 species) between the supercells of different sizes are negligible, as reported in Table S3. We thus used the smaller supercells throughout. The effect of the oxygen and hydroxyl species on propane adsorption is small on both surfaces (∼0.02 eV), while the propylene adsorption energy amounts to −0.73 and −0.95 eV on Pd(111) and Pd(211), respectively (see Figure 1 and Supporting Information).

We investigated propane dehydrogenation both on the clean Pd surfaces and in the presence of surface oxygen and hydroxyl

species. Scheme 1 shows the reaction mechanism and intermediates involved in both processes. The reaction involves two dehydrogenation steps: the first step is the conversion of propane (C_3H_8) into either 1 or 2 propyl (C_3H_7), followed by conversion into propylene (C_3H_6). In the oxygen (or OH) assisted DHP mechanism, a surface oxygen atom (or OH) abstracts the hydrogen from propane and its intermediates, forming hydroxyl (or water).

Mechanism of the Dehydrogenation of Propane (DHP) over Pd Surfaces. Free energy diagrams at a temperature of 600 °C are shown in Figure 2 along with

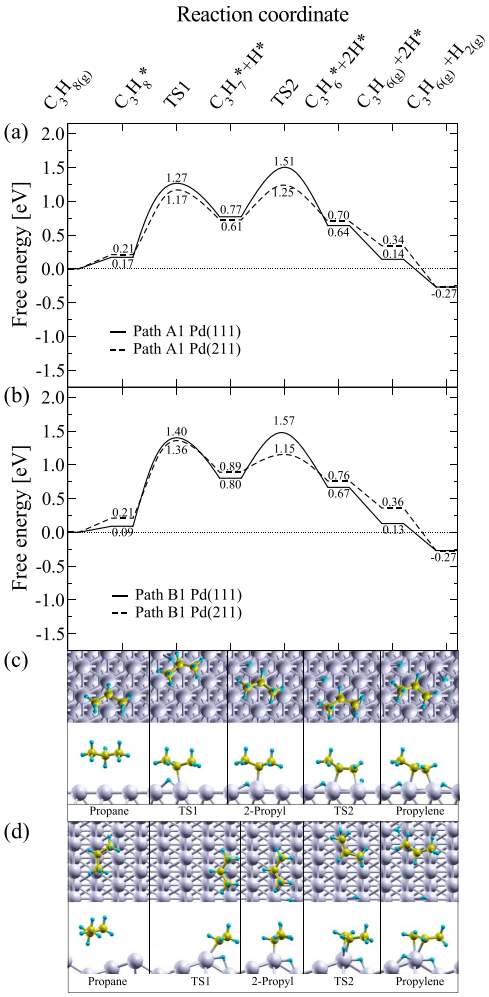

Figure 2. Free energy profile of DHP through (a) 1 propyl and (b) 2 propyl at 600 °C. Elementary steps of the pathway B1 over (c) Pd(111) and (d) Pd(211) surfaces.

structures of intermediates and transition states. We chose this temperature as this is typical for DHP.[7] Free energy profiles at a different temperature for selected pathways are presented in Figure S5. As can be seen in Figure 2a,b, the energy barriers for the first dehydrogenation step are slightly higher for path B, where 2 propyl is formed as an intermediate. It can also be seen that Pd(211) has slightly lower barriers, although the small differences compared to Pd(111) show that the structure sensitivity of this reaction is not pronounced as commonly observed for dehydrogenation reactions.[47] Interestingly, the energy barriers for the second dehydrogenation step are lower for Pd(211) compared to Pd(111) (see also Table S4). Relative to gas phase H_2, one can clearly see that the first dehydrogenation step constitutes the highest free energy barrier for both surfaces (see Figure S6). For Pd(211), both dehydrogenation barriers are quite similar, with the first barrier being lower for path A1 and higher for path B1. Finally, the desorption of both hydrogen and propylene involves no effort for both surfaces at 600 °C, indicating that the reaction takes place in the low coverage regime (within which all intermediates and reaction barriers have been calculated in the present study).

A comparison of the results obtained for Pd with those calculated for Pt (using the same functional and similar parameters) is shown in Figure S7.[28] Interestingly, while we find relatively small free energy barriers for the lowest energy pathways (1.10 and 0.96 eV for Pd(111) and Pd(211), respectively), these have been reported to be significantly higher on Pt surfaces (> 2.0 eV).[28]

Mechanism of ODHP over Pd Surfaces. The free energy profiles for the ODHP over both Pd surfaces are shown in Figure 3a,b and the elementary steps of the pathway B2 assuming a 2 propyl intermediate are presented in Figure 3c,d. Here, the first dehydrogenation step is O assisted (blue lines), while the second DH step is OH assisted (red lines). Interestingly, the differences in the two reaction pathways of the ODHP are negligible between both Pd surfaces. The

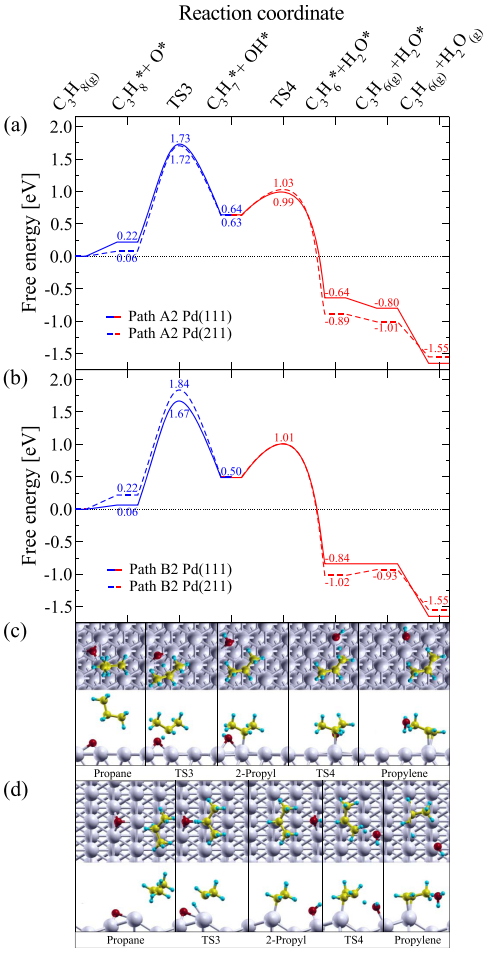

Figure 3. Free energy profile of ODHP through (a) 1 propyl and (b) a 2 propyl intermediate at 600 °C. Elementary steps of pathway B2 over (c) Pd(111) and (d) Pd(211) surfaces.

energy barriers of the first dehydrogenation step on the Pd surfaces are over 1.5 eV, 0.2−0.4 eV higher than the corresponding energy barriers for the direct DH process. The energy barrier of the second DH step is much lower: for the Pd(111) surface, around 0.7 eV for the direct route, and around 0.4 eV for the ODPH. For the Pd(211) surface, in the second DH step for ODHP, the energy barriers are slightly higher than those over the Pd(111) surface, which is in clear contrast with the direct route.

The previous results are further elaborated in Figure 4. If the first DH step proceeds via an OH assisted pathway, the

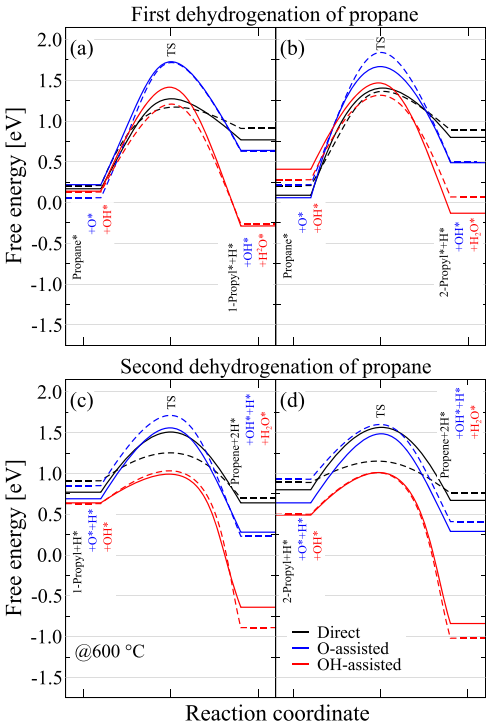

Figure 4. Direct, O , and OH assisted dehydrogenation of propane through (a) 1 propyl and (b) a 2 propyl intermediate; and dehydrogenation of (c) 1 propyl and (d) 2 propyl intermediates. Solid/dashed lines correspond to Pd(111)/Pd(211) surfaces.

activation energies are comparable to the direct DHP (but the final states are always lower in energy), and the O assisted steps are higher in energy barriers (Figure 4a,b). On the other hand, for the second DH step, it is clear that OH assisted DH has the lowest energy barriers, while the barriers for direct and O assisted DH steps are comparable (Figure 4c,d).

Figure 5 correlates the transition state energies (ΔE_{TS}) of all dehydrogenation steps expressed as a function of the final state energies (ΔE_{FS}) for reactions on clean, O* , and OH* covered surfaces (the reference energy levels are defined as shown in Figure S2). The solid lines represent scaling relations between the transition state of methane activation calculated for clean (black), O* (blue), and OH* covered (red) transition metal (111) surfaces as described in an earlier study.[48] We note that this study utilized the RPBE[49] functional, hence not accounting for dispersion forces. We performed single point calculations using the PBE + D3[38,39] functional to extract the D3 dispersion contributions of the final and transition states. We find that transition and final states are stabilized by roughly the same amount (about 0.55 eV; see Table S5). We therefore assume that the results of DHP and ODHP can be compared

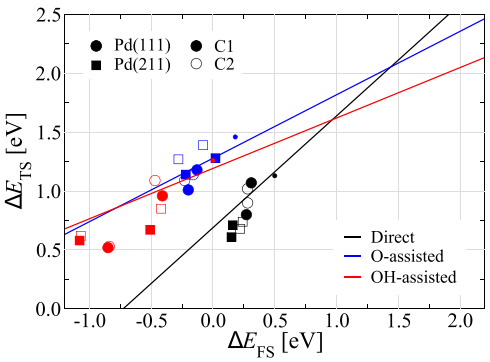

Figure 5. Transition state scaling relations for $C_3H_{8(g)}$ dehydrogenation on clean, O* covered, and OH* covered Pd(111) surfaces. Filled circles/squares, dehydrogenation from C1 carbon on Pd(111)/Pd(211) surfaces; open circles/squares, dehydrogenation from C2 carbon on Pd(111)/Pd(211) surfaces. Solid lines and small circles were taken from Yoo et al.[48] for CH_4 activation on transition metals (111) and Pd(111) surfaces, respectively. Figure S9 shows the difference in ΔE_{TS} between the O or OH assisted, and the direct DHP as a function of the difference in ΔE_{FS}.

to those calculated for CH_4 activation and be plotted against the corresponding transition state scaling (TSS) relations. The reason for the differences in correlations between ΔE_{TS} and ΔE_{FS} on clean transition metal surfaces and oxygen assisted dehydrogenation is due to the different transition state scaling lines for dehydrogenation. These phenomena can be explained by compensation effects as has been described earlier.[50]

Interestingly, despite the use of different functionals, propane dehydrogenation follows almost the same scaling relation determined for methane dehydrogenation over (111) transition metal surfaces (rescaled relations are presented in Figure S8), indicative of a more general scaling relation independent of the functional used or the C_xH_y species considered.[51] Apparently, these results can also be extended to propane dehydrogenation over (211) transition metal surfaces, but further studies are needed.

Figure 5 shows that the O assisted DHP has overall higher dehydrogenation barriers when compared with the direct dehydrogenation for Pd surfaces, even though the ΔE_{FS} is lower in energy; independently of the DH step and the position of the carbon from where the hydrogen is subtracted, O* does not favor DHP, as can be seen in Figure S9. On average, the OH assisted dehydrogenation has the lowest activation energy but also the lowest final state energies, suggesting strong exothermicity. Here, the first (at ca. −0.5 eV) and the second (at ca. −1.0 eV) DH steps can be identified, wherein the first DH steps have comparable ΔE_{TS} to the direct DHP but lower ΔE_{FS}, whereas the second DH steps have the lowest ΔE_{TS} and ΔE_{FS}.

This analysis shows that while surface oxygen coverage will decrease the activity of palladium toward DHP, there might be an improvement overall when surface hydroxyl groups participate in the reaction. The extent to which this promotional effect of hydroxyl dominates the overall reaction mechanism depends crucially on the OH* coverage (and the corresponding coverage of O*). These coverages in turn depend on the type of oxidant used and the corresponding reaction conditions. A detailed analysis of the steady state coverages, however, is only possible with elaborate micro kinetic models.

CONCLUSIONS

The reaction mechanisms of the (oxidative) dehydrogenation of propane to propylene over palladium surfaces were analyzed using DFT calculations. Interestingly, a comparison with literature data obtained for Pt surfaces indicates that Pd catalysts are more active for this reaction. We also found that the energy barriers of the oxidative dehydrogenation steps are always higher than those for the nonoxidative route. This strongly indicates that oxygen does not considerably change the kinetics of this reaction on Pd surfaces. We furthermore showed that the transition state energy scales with the final state energy (on Pd(111) and Pd(211) surfaces), both for the oxidative and for nonoxidative dehydrogenation, in analogy to an earlier study on methane activation. To fully explore the potential of Pd based catalysts, further studies concerning side reactions and catalyst deactivation would be needed.

AUTHOR INFORMATION

Corresponding Author

Felix Studt − *Karlsruhe Institute of Technology, Eggenstein-Leopoldshafen, Germany;* orcid.org/0000-0001-6841-4232; Email: felix.studt@kit.edu

Other Authors

Eduard Araujo-Lopez − *Karlsruhe Institute of Technology, Eggenstein-Leopoldshafen, Germany;* orcid.org/0000-0003-2063-1523

Lennart Joos − *Total Research & Technology Feluy, Seneffe, Belgium*

Bart D. Vandegehuchte − *Total Research & Technology Feluy, Seneffe, Belgium*

Dmitry I. Sharapa − *Karlsruhe Institute of Technology, Eggenstein-Leopoldshafen, Germany;* orcid.org/0000-0001-9510-9081

Complete contact information is available at: https://pubs.acs.org/10.1021/acs.jpcc.9b11424

Author Contributions

The manuscript was written through the contributions of all of the authors. All of the authors have given approval to the final version of the manuscript

Notes

The authors declare no competing financial interest.

ACKNOWLEDGMENTS

This work is part of the Consortium on Metal Nanocatalysis funded by Total Refining & Chemicals and it was supported by the Research Program Agreement, with reference Total/IPA 544 between Total Research & Technology Feluy and KIT.

REFERENCES

(1) Plotkin, J. S. The Changing Dynamics of Olefin Supply/Demand. *Catal. Today* **2005**, *106*, 10−14.

(2) Plotkin, J. S. The Propylene Gap: How Can It Be Filled? https://www.acs.org/content/acs//en/pressroom/cutting edge chemistry/the propylene gap how can it be filled.html.

(3) Chen, C.; Zhang, J.; Zhang, B.; Yu, C.; Peng, F.; Su, D. Revealing the Enhanced Catalytic Activity of Nitrogen Doped Carbon Nano tubes for Oxidative Dehydrogenation of Propane. *Chem. Commun.* **2013**, *49*, 8151.

(4) James, O. O.; Mandal, S.; Alele, N.; Chowdhury, B.; Maity, S. Lower Alkanes Dehydrogenation: Strategies and Reaction Routes to Corresponding Alkenes. *Fuel Process. Technol.* **2016**, *149*, 239−255.

(5) Wang, S.; Zhu, Z. H. Catalytic Conversion of Alkanes to Olefins by Carbon Dioxide Oxidative Dehydrogenation A Review. *Energy Fuels* **2004**, *18*, 1126−1139.

(6) Ansari, M. B.; Park, S. E. Carbon Dioxide Utilization as a Soft Oxidant and Promoter in Catalysis. *Energy Environ. Sci.* **2012**, *5*, 9419.

(7) Sattler, J. J. H. B.; Ruiz Martinez, J.; Santillan Jimenez, E.; Weckhuysen, B. M. Catalytic Dehydrogenation of Light Alkanes on Metals and Metal Oxides. *Chem. Rev.* **2014**, *114*, 10613−10653.

(8) Atanga, M. A.; Rezaei, F.; Jawad, A.; Fitch, M.; Rownaghi, A. A. Oxidative Dehydrogenation of Propane to Propylene with Carbon Dioxide. *Appl. Catal., B* **2018**, *220*, 429−445.

(9) Cai, W.; Mu, R.; Zha, S.; Sun, G.; Chen, S.; Zhao, Z. J.; Li, H.; Tian, H.; Tang, Y.; Tao, F.; et al. Subsurface Catalysis Mediated Selectivity of Dehydrogenation Reaction. *Sci. Adv.* **2018**, *4*, No. eaar5418.

(10) Kaylor, N.; Davis, R. J. Propane Dehydrogenation over Supported Pt Sn Nanoparticles. *J. Catal.* **2018**, *367*, 181−193.

(11) Saelee, T.; Namuangruk, S.; Kungwan, N.; Junkaew, A. Theoretical Insight into Catalytic Propane Dehydrogenation on Ni(111). *J. Phys. Chem. C* **2018**, *122*, 14678−14690.

(12) Yan, Z.; Goodman, D. W. Silica Supported Au−Ni Catalysts for the Dehydrogenation of Propane. *Catal. Lett.* **2012**, *142*, 517−520.

(13) Nowicka, E.; Reece, C.; Althahban, S. M.; Mohammed, K. M. H.; Kondrat, S. A.; Morgan, D. J.; He, Q.; Willock, D. J.; Golunski, S.; Kiely, C. J.; et al. Elucidating the Role of CO_2 in the Soft Oxidative Dehydrogenation of Propane over Ceria Based Catalysts. *ACS Catal.* **2018**, *8*, 3454−3468.

(14) Yang, C.; Wu, Z.; Zhang, G.; Sheng, H.; Tian, J.; Duan, Z.; Sohn, H.; Kropf, A. J.; Wu, T.; Krause, T. R.; et al. Promotion of Pd Nanoparticles by Fe and Formation of a Pd_3Fe Intermetallic Alloy for Propane Dehydrogenation. *Catal. Today* **2019**, *323*, 123−128.

(15) Mentasty, L. R.; Gorriz, O. F.; Cadus, L. E. Chromium Oxide Supported on Different Al_2O_3 Supports: Catalytic Propane Dehydro genation. *Ind. Eng. Chem. Res.* **1999**, *38*, 396−404.

(16) Fu, H.; Liu, Z. P.; Li, Z. H.; Wang, W. N.; Fan, K. N. Periodic Density Functional Theory Study of Propane Oxidative Dehydrogen ation over V_2O_5 (001) Surface. *J. Am. Chem. Soc.* **2006**, *128*, 11114−11123.

(17) Sandupatla, A. S.; Nayak, S. C.; Sivananda, C.; Deo, G. DFT Investigation into the Experimentally Observed Influence of Oxide Support in the ODH of Propane over Supported Vanadia Catalysts. *Catal. Today* **2019**, *325*, 18−24.

(18) Michorczyk, P.; Ogonowski, J. Dehydrogenation of Propane in the Presence of Carbon Dioxide over Oxide Based Catalysts. *React. Kinet. Catal. Lett.* **2003**, *78*, 41−47.

(19) Larsson, R. Propane Dehydrogenation Catalyzed by ZSM 5 Zeolites. A Mechanistic Study Based on the Selective Energy Transfer (SET) Theory. *Molecules* **2015**, *20*, 2529−2535.

(20) Sun, G.; Zhao, Z. J.; Mu, R.; Zha, S.; Li, L.; Chen, S.; Zang, K.; Luo, J.; Li, Z.; Purdy, S. C.; et al. Breaking the Scaling Relationship via Thermally Stable Pt/Cu Single Atom Alloys for Catalytic Dehydro genation. *Nat. Commun.* **2018**, *9*, No. 4454.

(21) Hu, W.; Cao, X. Monitoring Reaction Paths Using Vibrational Spectroscopies: The Case of the Dehydrogenation of Propane toward Propylene on Pd Doped Cu(111) Surface. *Molecules* **2018**, *23*, 126.

(22) Gallagher, J. R.; Childers, D. J.; Zhao, H.; Winans, R. E.; Meyer, R. J.; Miller, J. T. Structural Evolution of an Intermetallic Pd−Zn Catalyst Selective for Propane Dehydrogenation. *Phys. Chem. Chem. Phys.* **2015**, *17*, 28144−28153.
(23) Childers, D. J.; Schweitzer, N. M.; Shahari, S. M. K.; Rioux, R. M.; Miller, J. T.; Meyer, R. J. Modifying Structure Sensitive Reactions by Addition of Zn to Pd. *J. Catal.* **2014**, *318*, 75−84.
(24) Wu, Z.; Wegener, E. C.; Tseng, H. T.; Gallagher, J. R.; Harris, J. W.; Diaz, R. E.; Ren, Y.; Ribeiro, F. H.; Miller, J. T. Pd−In Intermetallic Alloy Nanoparticles: Highly Selective Ethane Dehydro genation Catalysts. *Catal. Sci. Technol.* **2016**, *6*, 6965−6976.
(25) Yang, M. L.; Zhu, Y. A.; Zhou, X. G.; Sui, Z. J.; Chen, D. First Principles Calculations of Propane Dehydrogenation over PtSn Catalysts. *ACS Catal.* **2012**, *2*, 1247−1258.
(26) Yang, M. L.; Zhu, Y. A.; Fan, C.; Sui, Z. J.; Chen, D.; Zhou, X. G. DFT Study of Propane Dehydrogenation on Pt Catalyst: Effects of Step Sites. *Phys. Chem. Chem. Phys.* **2011**, *13*, 3257−3267.
(27) Yang, M. L.; Zhu, Y. A.; Zhou, X. G.; Sui, Z. J.; Chen, D. First Principles Calculations of Propane Dehydrogenation over PtSn Catalysts. *ACS Catal.* **2012**, *2*, 1247−1258.
(28) Zha, S.; Sun, G.; Wu, T.; Zhao, J.; Zhao, Z. J.; Gong, J. Identification of Pt Based Catalysts for Propane Dehydrogenation via a Probability Analysis. *Chem. Sci.* **2018**, *9*, 3925−3931.
(29) Kresse, G.; Furthmüller, J. Efficient Iterative Schemes for Ab Initio Total Energy Calculations Using a Plane Wave Basis Set. *Phys. Rev. B* **1996**, *54*, No. 11169.
(30) Kresse, G.; Furthmüller, J. Efficiency of Ab Initio Total Energy Calculations for Metals and Semiconductors Using a Plane Wave Basis Set. *Comput. Mater. Sci.* **1996**, *6*, 15−50.
(31) Larsen, A. H.; Mortensen, J. J.; Blomqvist, J.; Castelli, I. E.; Christensen, R.; Dułak, M.; Friis, J.; Groves, M. N.; Hammer, B.; Hargus, C.; et al. The Atomic Simulation Environment—a Python Library for Working with Atoms. *J. Phys.: Condens. Matter* **2017**, *29*, No. 273002.
(32) Mortensen, J. J.; Kaasbjerg, K.; Frederiksen, S. L.; Nørskov, J. K.; Sethna, J. P.; Jacobsen, K. W. Bayesian Error Estimation in Density Functional Theory. *Phys. Rev. Lett.* **2005**, *95*, No. 216401.
(33) Wellendorff, J.; Lundgaard, K. T.; Møgelhøj, A.; Petzold, V.; Landis, D. D.; Nørskov, J. K.; Bligaard, T.; Jacobsen, K. W. Density Functionals for Surface Science: Exchange Correlation Model Development with Bayesian Error Estimation. *Phys. Rev. B* **2012**, *85*, No. 235149.
(34) Blöchl, P. E. Projector Augmented Wave Method. *Phys. Rev. B* **1994**, *50*, No. 17953.
(35) Kresse, G.; Joubert, D. From Ultrasoft Pseudopotentials to the Projector Augmented Wave Method. *Phys. Rev. B* **1999**, *59*, No. 1758.
(36) Wellendorff, J.; Silbaugh, T. L.; Garcia Pintos, D.; Nørskov, J. K.; Bligaard, T.; Studt, F.; Campbell, C. T. A Benchmark Database for Adsorption Bond Energies to Transition Metal Surfaces and Comparison to Selected DFT Functionals. *Surf. Sci.* **2015**, *640*, 36−44.
(37) Sharada, S. M.; Bligaard, T.; Luntz, A. C.; Kroes, G. J.; Nørskov, J. K. SBH10: A Benchmark Database of Barrier Heights on Transition Metal Surfaces. *J. Phys. Chem. C* **2017**, *121*, 19807−19815.
(38) Perdew, J. P.; Burke, K.; Ernzerhof, M. Generalized Gradient Approximation Made Simple. *Phys. Rev. Lett.* **1996**, *77*, No. 3865.
(39) Grimme, S.; Antony, J.; Ehrlich, S.; Krieg, H. A Consistent and Accurate Ab Initio Parametrization of Density Functional Dispersion Correction (DFT D) for the 94 Elements H Pu. *J. Chem. Phys.* **2010**, *132*, No. 154104.
(40) Henkelman, G.; Jónsson, H. Improved Tangent Estimate in the Nudged Elastic Band Method for Finding Minimum Energy Paths and Saddle Points. *J. Chem. Phys.* **2000**, *113*, 9978−9985.
(41) Henkelman, G.; Jónsson, H. A Dimer Method for Finding Saddle Points on High Dimensional Potential Surfaces Using Only First Derivatives. *J. Chem. Phys.* **1999**, *111*, 7010−7022.
(42) Afeefy, H. Y.; Liebman, J. F.; Stein, S. E. Neutral Thermochemical Data. In *NIST Chemistry WebBook. NIST Standard Reference Database Number 69*; Linstrom, P. J.; Mallard, W. G., Eds.; National Institute of Standards and Technology: Gaithersburg, MD, 2019; http://webbook.nist.gov.
(43) Chao, J.; Wilhoit, R. C.; Zwolinski, B. J. Ideal Gas Thermodynamic Properties of Ethane and Propane. *J. Phys. Chem. Ref. Data* **1973**, *2*, 427−438.
(44) Chao, J.; Zwolinski, B. J. Ideal Gas Thermodynamic Properties of Ethylene and Propylene. *J. Phys. Chem. Ref. Data* **1975**, *4*, 251−262.
(45) Weaver, J. F.; Hakanoglu, C.; Hawkins, J. M.; Asthagiri, A. Molecular Adsorption of Small Alkanes on a PdO(101) Thin Film: Evidence of σ Complex Formation. *J. Chem. Phys.* **2010**, *132*, No. 024709.
(46) Tait, S. L.; Dohnálek, Z.; Campbell, C. T.; Kay, B. D. N Alkanes on Pt(111) and on C(0001)/Pt(111): Chain Length Dependence of Kinetic Desorption Parameters. *J. Chem. Phys.* **2006**, *125*, No. 234308.
(47) Wang, S.; Petzold, V.; Tripkovic, V.; Kleis, J.; Howalt, J. G.; Skúlason, E.; Fernández, E. M.; Hvolbæk, B.; Jones, G.; Toftelund, A.; et al. Universal Transition State Scaling Relations for (de) Hydrogenation over Transition Metals. *Phys. Chem. Chem. Phys.* **2011**, *13*, 20760.
(48) Yoo, J. S.; Khan, T. S.; Abild Pedersen, F.; Nørskov, J. K.; Studt, F. On the Role of the Surface Oxygen Species during A−H (A = C, N, O) Bond Activation: A Density Functional Theory Study. *Chem. Commun.* **2015**, *51*, 2621−2624.
(49) Hammer, B.; Hansen, L. B.; Nørskov, J. K. Improved Adsorption Energetics within Density Functional Theory Using Revised Perdew Burke Ernzerhof Functionals. *Phys. Rev. B* **1999**, *59*, No. 7413.
(50) Tsai, C.; Latimer, A. A.; Yoo, J. S.; Studt, F.; Abild Pedersen, F. Predicting Promoter Induced Bond Activation on Solid Catalysts Using Elementary Bond Orders. *J. Phys. Chem. Lett.* **2015**, *6*, 3670−3674.
(51) Garcia Pintos, D.; Voss, J.; Jensen, A. D.; Studt, F. Hydrodeoxygenation of Phenol to Benzene and Cyclohexane on Rh(111) and Rh(211) Surfaces: Insights from Density Functional Theory. *J. Phys. Chem. C* **2016**, *120*, 18529−18537.